ResearchGate

See discussions, stats, and author profiles for this publication at: https://www.researchgate.net/publication/231398380

Effects of stirring on photoinduced phase transition in a batch-mode Briggs-Rauscher reaction

ARTICLE *in* THE JOURNAL OF PHYSICAL CHEMISTRY · MARCH 1993

Impact Factor: 2.78 · DOI: 10.1021/j100111a028

CITATIONS
15

READS
35

2 AUTHORS, INCLUDING:

Vladimir K Vanag
Immanuel Kant Baltic Federal University
78 PUBLICATIONS **2,108** CITATIONS

SEE PROFILE

Available from: Vladimir K Vanag
Retrieved on: 22 January 2016

THE JOURNAL OF
PHYSICAL CHEMISTRY

Subscriber access provided by BRANDEIS UNIV

Effects of stirring on photoinduced phase transition in a batch-mode Briggs-Rauscher reaction

Vladimir K. Vanag, and Michail V. Alfimov

J. Phys. Chem., **1993**, 97 (9), 1884-1890 • DOI: 10.1021/j100111a028

Downloaded from http://pubs.acs.org on January 14, 2009

More About This Article

The permalink http://dx.doi.org/10.1021/j100111a028 provides access to:

- Links to articles and content related to this article
- Copyright permission to reproduce figures and/or text from this article

ACS Publications
High quality. High impact.

The Journal of Physical Chemistry is published by the American Chemical Society. 1155 Sixteenth Street N.W., Washington, DC 20036

Effects of Stirring on Photoinduced Phase Transition in a Batch-Mode Briggs–Rauscher Reaction

Vladimir K. Vanag* and Michail V. Alfimov

Department of Photochemistry, N. N. Semenov Institute of Chemical Physics, Russian Academy of Sciences, 117421, Novatorov Str., 7A, Moscow, Russia

Received: June 29, 1992; In Final Form: October 12, 1992

With a batch-operated Briggs–Rauscher reaction, a study has been made of the effects of stirring on the photoinduced kinetic phase transition from the quasi-steady state (I) with low iodine and iodide concentrations to the quasi-steady state (II) with high $[I_2]$ and $[I^-]$. It is shown that the time T_{ill} from the moment of switching on the light to the moment of the I → II transition increases with increasing Reynolds number. At certain light intensities, T_{ill} at $Re \cong 200$–4000 is 5–10 times shorter than T_{ill} at $Re \cong 10\,000$–$12\,000$. The dependence of T_{ill} on Re is S-shaped. This dependence is shown to be associated with formation of nuclei of state II in state I of the Briggs–Rauscher reaction. The results obtained are discussed on the basis of the relationships between the kinetic characteristics of the chemistry and the hydrodynamic characteristics of turbulence and mass transfer. Estimates are given for the characteristic sizes and lifespans of the nuclei.

1. Introduction

Quite a number of works[1-22] have been devoted to the effects of stirring on nonlinear dynamic chemical systems, in particular on autocatalytic and oscillatory reactions. Yet there is still no consensus on how the stirring intensity affects homogeneous chemical reactions displaying instabilities, multistabilities, oscillations, and chaos.

Frank-Kamenetskii[1] was one of the first to recognize the importance of diffusion and mass mixing in chemical kinetics. After him the influence of stirring on oscillatory reactions was also studied by the discoverers of homogeneous chemical oscillators.[2] Using point Pt electrodes, they have shown that in a nonstirred batch reactor at certain initial reagent concentrations the Belousov–Zhabotinskii (BZ) reaction may proceed in a mode when microoscillators exist in every point of the reaction volume but there are no bulk macrooscillations. The cause of this is the lack of phase coupling between the microoscillators. At the same time, stirring gives rise to macrooscillations, which can be interpreted as synchronization of a large number of microoscillators.

An opposite effect has been observed in work[3] where authors suppose that chaotic oscillations in the BZ reaction in a continuous-flow stirred tank reactor (CSTR) are due to imperfect mixing of the feedstreams into the bulk of the reaction mixture, and result from coupling among regions of somewhat different chemical composition developing in different parts of the CSTR. The influence of imperfect mixing which creates heterogeneities affecting the nonequilibrium phase transitions in dynamic systems studied in CSTR has been found in quite a few works.[4-10,13,16,17,19-21] Most of these effects can be explained in terms of a nonideal reactor that can be mimicked by two or more ideal CSTRs coupled through mass transfer and can be (partly) obviated by premixing.

The studies on stirring effects in batch reactors[2,11,12,14,15,18,22] are at first glance free of such a drawback as imperfect mixing and are more interesting in this respect. However, in some of these works carried out with open batch reactors the influence of stirring on chemical instabilities (manifesting itself, e.g., as changes in the frequency and amplitude of oscillations in the BZ reaction) were explained, albiet not completely, by gas exchange with the atmosphere, in particular by the action of the atmospheric oxygen.

Besides these two causes, two more possibilities of stirring effects in chemical reactions are discussed in the literature.[18,22] These are adsorption processes on the wall of a batch reactor, and surface catalytic processes at a Pt electrode. Further, it has been mentioned[21] that stirring effects can be considered in the framework of the influence of external noise on phase transitions in nonequilibrium systems.[23,24] However, this approach has not yet been followed up or supported experimentally. Most of the studies concerning stirring effects have been conducted on the BZ reaction and some on the chlorite/iodide reaction.

In this work we present experimental data on the effects of stirring on chemical instabilities in the Briggs–Rauscher (BR) reaction in a well-stirred batch reactor. As shown in our previous works,[25-27] in this system under certain initial conditions the BR reaction after the end of oscillations may undergo a kinetic (or nonequilibrium) phase transition from state I with low concentrations of I_2 and I^- to state II with high I_2 and I^- concentrations. This transition can be evoked by additions of iodide at 10^{-6} M and higher[25] or by light (both in the UV and in the visible ranges). It has also been demonstrated[26,27] that the dependence of the response of the BR system in state I on the dosage of illumination at fixed light intensity is of a threshold type, and that the I → II transition proceeds with an exponential rise in $[I_2]$ and $[I^-]$.

All this indicates that the I → II transition is a saddle-node bifurcation that is in many aspects analogous to an equilibrium first-order transition. The latter is known[28,29] to differ from the second-order transition in that it proceeds via a nucleation mechanism. In this work, by studying how the exposure to light necessary for the transition depends on the stirring intensity, we have tried to determine (i) whether there are nuclei of phase II in state I of the system during the I → II transition, and (ii) if there are, what are their characteristic size and lifespan.

2. Materials and Methods

The reagents malonic acid (MA), KIO_3, $Mn(NO_3)_2{\cdot}6H_2O$, KI, H_2O_2, and H_2SO_4 were of analytical grade; hydrogen peroxide was stabilizer-free. All solutions were prepared in distilled water. Stock solutions were stored in glass stoppered bottles protected from light.

Absorptivities (M^{-1} cm^{-1}) used were for $[I_2]$ $\epsilon_{463} = 746$, for $[I_3^-]$ $\epsilon_{360} = 25000$ and $\epsilon_{463} = 975$, and for iodomalonic acid (IMA) $\epsilon_{350} = 14.8$[30,31] and $\epsilon_{360} = 9$.[25]

The course of the reaction was followed by monitoring $[I_2]$ by absorbance at 463 nm, $[I^-]$ with a iodide-selective electrode, $[I_3^-]$ and malonic acid products by absorbance at 360 nm, as well as by recording the potential of a platinum electrode (U_{Pt}). The potentials of iodide-selective (U_I) and Pt electrodes were measured against an Ag–AgCl reference electrode connected to the reaction vessel via a Na_2SO_4 saturated salt bridge. The iodide-selective

0022-3654/93/2097-1884$04.00/0 © 1993 American Chemical Society

electrode was made by Ecotest (Moscow) on the basis of a pressed AgI/Ag_2S tablet. The characteristics of the iodide-selective electrode and of the spectrophotometric unit have been given in detail elsewhere.[25] The Pt electrode (Radelkis, Budapest) was made of a 0.5-mm-diameter platinum wire protruding 0.3 mm from a glass tube 6.5 mm in diameter. All electrode potentials were recorded using a U5-11 electrometric amplifier with an input resistance $R_{in} = 10^{11}$ Ω. This completely excluded the possible influence of the weak electrochemical current (on the order of $i = U_{Pt}/R_{in}$) on reagent concentrations. Indeed, at $U_{Pt} \cong 0.5$ V and $R_{in} = 10^{11}$ Ω the electrochemical oxidation of, e.g., iodide on the Pt electrode during a period $\Delta t \cong 100$ s cannot decrease its concentration by more than $\Delta ti/FV \cong 10^{-12}$ M (F is the faraday and V is the reaction volume).

The experiments were conducted in a batch thermostated cylindrical Teflon cell (i.d. 2 cm, $V = 10$ mL) with flat quartz windows press-fitted on four sides. Electrodes were inserted into the cell lid. In one series of experiments stirring was done with magnetically driven glass-coated bars rotating on the bottom of the vessel; the bars were 2 mm in diameter and 1–1.8 cm long. The rotation frequency varied from 5.4 to 11.1 Hz. In the other series use was made of a mechanical two-blade Teflon stirrer the upper edge of which was positioned 5 mm below the surface of solution. The stirred blade area was 1 × 1 cm²; the rotation frequency was varied from 2 to 35 Hz.

The Reynolds number was determined according to the equation $Re = ud/\nu_k$, where d is the stirrer length from tip to tip, u is the characteristic flow velocity ($u = f_0\pi d$, f_0 is the rotation frequency), and ν_k is the kinematic viscosity which for water is equal to 0.01 cm²/s at 25 °C. The efficiency and the pattern of mixing was assessed in two ways.

(1) A drop of dye 0.9 mm in diameter was carefully applied onto the surface of stirred water, and the rate of its spreading was determined from the change in absorbance. The absorbance vs time dependences thus obtained were approximated well enough with a function $C_1 \exp(-t/t_{mix}^{(1)}) \sin(\omega t) + C_2 \exp(-t/t_{mix}^{(2)})$. As expected, the ω values proved to correlated nicely with the stirrer frequency f_0, and $t_{mix}^{(1)}$ and $t_{mix}^{(2)}$ at the same Re number did not differ from more than 2–3-fold. For a monoparametric characteristic of the process of drop mixing, use was henceforth made of the value $t_{mix} = (t_{mix}^{(1)} t_{mix}^{(2)})^{1/2}$.

(2) Power spectra were determined for the photocurrent generated by the light scattered from microspheres of monodisperse latex suspended in water[32] at different Reynolds numbers. The light source was a helium/neon single mode laser ($P = 5$ mW, λ = 6328 Å). The polyacrolein and polystyrene latex microspheres had diameters of 0.7 and 1.8 μm;[33] aggregates of several microspheres could occur in the prepared dispersions. The scattered light was measured at a 90° angle in the same spectrophotometric unit that was used for the main experiments. The scattering volume was set by the thickness of the laser beam, (0.3 mm) and the width of a slit (0.25 mm) placed perpendicular to the beam at a distance of 4 cm from the cell center and was approximately equal to 0.02 mm³. Thus the observations were essentially local measurements and no significant spatial averaging was involved. The signal from the photomultiplier was supplied to an SK4-72/2 real-time spectrum analyzer.

The stirrer rotation frequency f_0 was determined in special experiments from the modulation of the signal of the photomultiplier picking up the light beam chopped by the stirrer and also from the position of the characteristic maximum in the power spectrum of scattered light.

The temperature was controlled with an accuracy of ±0.1 °C and varied from 20 to 27 °C.

3. Results. Microheterogeneities

Taking into account the results of our previous works[25,27] to obtain state I of the system the Briggs–Rauscher reaction is started

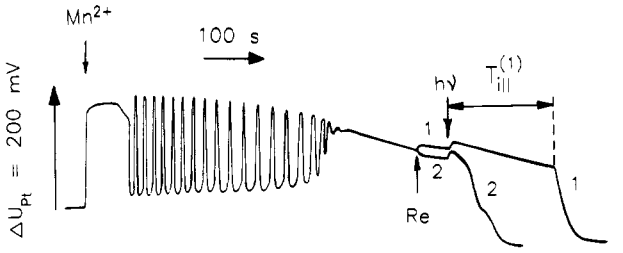

Figure 1. Kinetics of the Briggs–Rauscher reaction recorded as the platinum electrode potential U_{Pt}. The reaction is initiated at the mechanical stirrer frequency $f_0 = 21.6$ Hz ($Re_0 = 6770$); at the moment marked with arrow Re the stirrer frequency is changed to $f_1 = 33.1$ Hz in curve 1 and to $f_2 = 6.42$ Hz in curve 2. At the moment marked with arrow $h\nu$ the system is illuminated through an SZS-22 filter (380–540 nm); the incident light intensity is 12.8 mW. Reagent concentrations are given in the text.

in the oscillatory regime at the following initial reagent concentrations: $[H_2SO_4]_0 = 0.1$ M, $[H_2O_2]_0 = 0.61$ M, $[Mn^{2+}]_0 = 3.5 \times 10^{-2}$ M, $[MA]_0 = 6 \times 10^{-2}$, $[KIO_3]_0 = 2.25 \times 10^{-2}$ M. The typical reaction kinetics recorded with a Pt electrode is shown in Figure 1. After the end of oscillations, i.e., the O → I transition, in about 100 s the remaining iodate practically completely disappears from the system[25] and at the same time there is a pronounced increase in a diiodo derivative of malonic acid R_xI_2 (which is manifest in the rise in absorbance in the 350–360-nm band, Figure 2) while the concentrations of I_2 and I^- do not exceed 2×10^{-6} and 10^{-8} M, respectively. State I of the system is unstable because of the lability of R_xI_2. After a certain time τ, which is the lifespan of state I, the system may pass into state II. The I → II transition is the breakdown of R_xI_2 yielding I_2 and I^-;[25] in the onset of the transition $[I_2]$ and $[I^-]$ increase exponentially as $\exp(\gamma t)$ with a constant $\gamma = 0.2$–0.4 s⁻¹ (depending on temperature and initial concentrations) and finally reach values about 10^{-3} and 2×10^{-4} M, respectively.

The lifespan τ is quite strongly influenced by external factors such as stirring intensity and illumination. If the system is kept in the dark and vigorously stirred, the I → II transition does not take place at all ($\tau = \infty$) while R_xI_2 decomposes slowly but completely. If the stirring is weak, a spontaneous transition to state II takes place. Illumination of the system markedly shortens τ but only slightly, if at all, affects γ.[27] State I of the illuminated system can be characterized by two values: exponent γ, and the time from the start of illumination to the onset of the I → II transition, which we designate as T_{ill}. The dependence of T_{ill} on exposure $H = I_0 t_{ill}$ (where t_{ill} is illumination time and I_0 light intensity) is of a threshold type.[26,27]

To obtain the dependences of γ and T_{ill} on stirring intensity, the main group of experiments have been run as follows. The reaction was initiated at a certain fixed number Re_0 (6770 with the mechanical stirrer; 11 300 for $d = 1.8$ cm and 3750 for $d = 1.05$ cm with magnetic stirrer bars). After reaching maximal absorbance at 360 nm, a new Re value was set and 50 s later, when the new stirring regime was fully established, the system was exposed to light.

As shown in our preceding paper,[27] there are at least two photosensitive molecules in the system: I_2 and R_xI_2 which have different absorption bands and yield different photoreaction products:

$$R_xI_2 \xrightarrow{h\nu_1} R_xI^\bullet + I^\bullet \quad (1)$$

$$I_2 \xrightarrow{h\nu_2} 2I^\bullet \quad (2)$$

Visible light is mainly absorbed by iodine and partly by R_xI_2 owing to its spectral tailing, whereas ultraviolet light is mainly absorbed by R_xI_2. Therefore in one series of experiments the system was illuminated with blue light using an SZS-22 filter

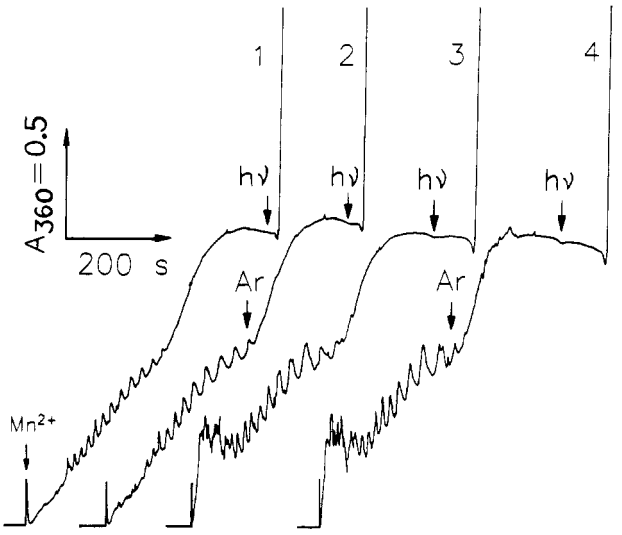

Figure 2. Kinetics of the Briggs–Rauscher reaction followed by the absorbance at 360 nm. Curves 1 and 2, stirring with glass-coated magnetic stirrer bar 1.8 cm long and 2 mm in diameter at Re = 5530 and Re = 11 300, respectively; curves 3 and 4, with Teflon-coated bar 1.3 cm long and 8 mm in diameter, Re = 5900; t = 20 °C, V_0 = 8 mL. Arrows Ar mark the moments when a flow of argon is directed into the cell, arrows $h\nu$ mark the switch on of white light with an intensity of 52.8 mW.

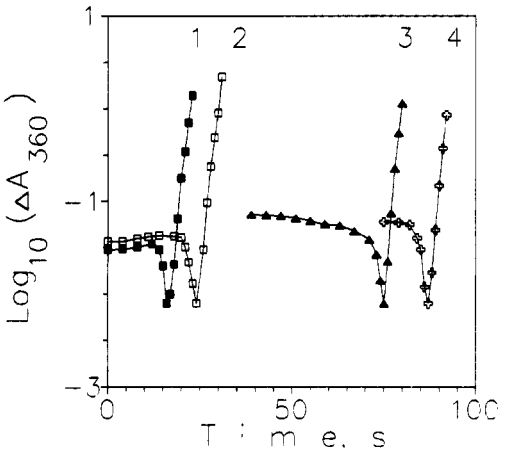

Figure 3. Fragments of the kinetics of the Briggs–Rauscher reaction from Figure 2 (numbering is the same) presented as plots of log ΔA_{360} vs t. The moment t = 0 corresponds to light switch on; $\Delta A_{360} = A_t - A_{min} + C$, where A_t is the current absorbance at 360 nm at time t, A_{min} is the minimal value of A_{360} after switching on the light, $C \cong 0.01$.

with transmission half-peak width 380–540 nm; in another series illumination was with white light, which significantly enhanced the contribution of photoreaction (1) to the induction of the I → II transition.

Our experiments have revealed that the exponent γ is virtually independent of the stirring intensity; this is illustrated by typical kinetic curves in Figure 3.

Figures 4–6 present the dependences of T_{ill} and threshold exposure $H_{thr} = I_0 T_{ill}$ on Re for two stirrer types (magnetic and mechanical), for different spectral regions of the photolyzing light and for its different intensities I_0. The $H_{thr}(Re)$ dependences are given instead of $T_{ill}(Re)$ to make it possible to compare curves obtained at different light intensities (I_0 was varied using neutral density filters (metal grids) with an attenuation factor of 2.27 and was assumed to be equal to unity without such filters).

As can be seen, a feature common to these dependences is their sigmoid shape. Thus under blue light (Figure 4) there are two regions of Re values where T_{ill} only slightly changes (Re < 2000 and Re > 10,000) whereas between them the response is quite pronounced.

Illumination with white light exhibits another peculiarity, namely the "stretching" of the high-response range toward higher

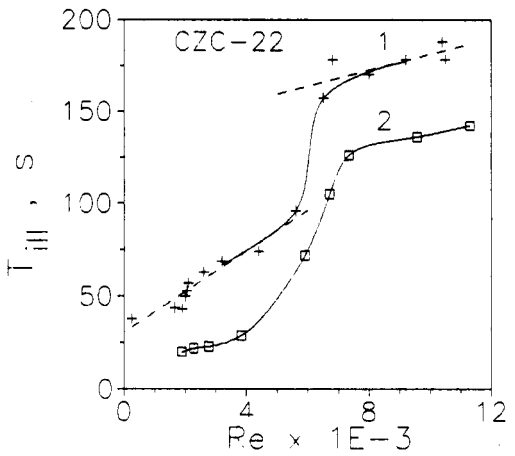

Figure 4. Dependences of the threshold illumination time T_{ill} on Re for the case of illumination of state I of the Briggs–Rauscher system with blue light of incident intensity 12.8 mW. Curve 1, mechanical stirrer; curve 2, glass-coated magnetic stirrer bars. For curve 1 the groups of data to the left and to the right of Re = 6000 are approximated with straight lines using the method of least-squares. 1E–3 ≡ 10^{-3}.

Re at reduced light intensity; this is observed with both mechanical and magnetic stirrers (confer curves 1 and 2 in Figures 5 and 6). No such effect can be found under blue light.

Figures 5 and 6 further show that the threshold exposures H_{thr} for different I_0 are rather close at low Re but substantially diverge at higher Re. Using the data of the preceding work[27] that allow the I_0 values for light of different spectral composition to be recalculated into the rates of generation of radicals R• (R• = I•, R_xI•), we have obtained the dependences of $[R^\bullet]_{thr}$ on $d[R^\bullet]/dt$, where $[R^\bullet]_{thr} = T_{ill}\, d[R^\bullet]/dt$ is the threshold integral concentration of the radicals necessary for the I → II transition to take place. Figure 7 demonstrates that at high Re the $[R^\bullet]_{thr}$ value is greatly dependent on the radical photogeneration rate $d[R^\bullet]/dt$.

A question naturally arising is whether the stirring effect can be due to gas exchange between the air and the solution and to reaction between oxygen and the intermediates formed under illumination: R_xI•, I•, MA•, IMA•, etc. On the strength of the results of special experiments described in the Appendix, we can rule out this suggestion.

Also invalid is the hypothesis that the active radicals initiating the I → II transition may perish on the reactor walls, and the more intense is the stirring the faster they reach the walls and thus the more massively they are eliminated. This mechanism is well-known in the gaseous phase[34] but is practically impossible in liquids, since the life time τ_R of a radical dictated by its chemical reactions is far shorter than the time τ_d of its delivery to the wall. Thus, for instance, for radical I• which plays a decisive part in the I → II transition the life time τ_R is limited by reaction 3:

$$I^\bullet + H_2O_2 \xrightarrow{k_3} HOI + OH^\bullet \qquad (3)$$

where $k_3 \cong 5 \times 10^7$ M^{-1} s^{-1} (ref 35) and accordingly $\tau_R \leq (k_3[H_2O_2])^{-1} \cong 0.3 \times 10^{-7}$ s, whereas $\tau_d \cong d/u \cong 0.01$–$0.1$ s.

It must also be pointed out that the effect of stirring cannot be explained by heterogeneous catalysis of some reactions on solid surfaces of the electrodes, because dependences analogous to those depicted in Figures 4–7 have been obtained without using electrodes.

Thus, the dependences of H_{thr} on Re, T_{ill} on Re, and $[R^\bullet]_{thr}$ on $d[R^\bullet]/dt$ presented in Figures 4–7 can be considered indicative of the existence of heterogeneities in solution, which may be the nuclei of the new phase, i.e., microvolumes in which the I → II transition has started. The explanation for such dependences should be sought in the interrelationship between the hydrodynamic characteristics of the stirred liquid and the kinetic characteristics of the chemical reactions.

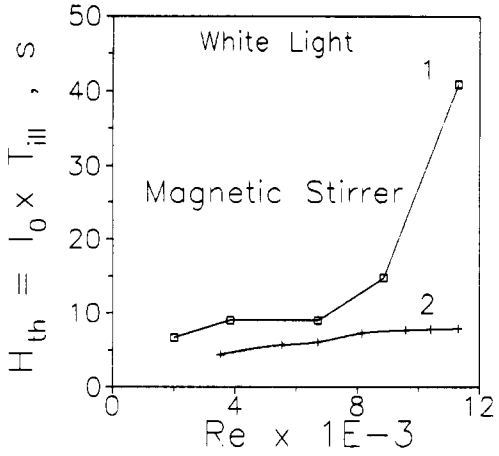

Figure 5. Dependences of the threshold exposure $H_{thr} = I_0 T_{ill}$ on Re for state I of the Briggs–Rauscher system illuminated with white light; curve 1, I_0 = 0.44 (52.8 mW); curve 2, I_0 = 1 (120 mW). Magnetic stirrer, glass-coated bars.

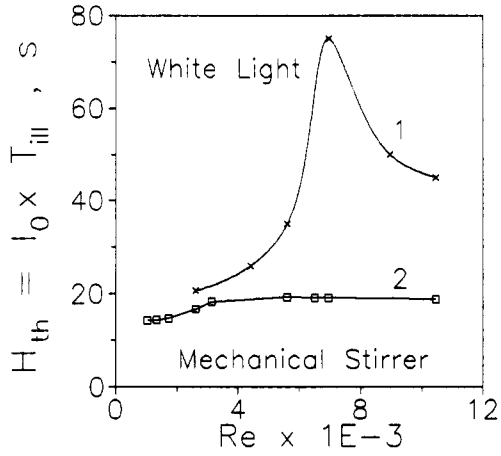

Figure 6. Dependences of the threshold exposure H_{thr} on Re similar to those in Figure 5 but with a mechanical Teflon stirrer.

However, besides microheterogeneities, nonequilibrium dynamic systems may contain macroheterogeneities, i.e., macrogradients of some substance(s). Menzinger and co-workers[18,19] have found such macrogradients in the chlorite/iodide and the BZ reaction using a Pt microelectrode, whose potential proved to depend on the stirring intensity and the electrode position. As to our case, we have shown,[27] by altering the cross section of the incident light beam with the SI_0 product held constant, that the reaction mixture is macrohomogeneous. Yet we have also observed changes in U_{Pt} with changing Re (see Figure 1). With increasing Re the potential rises by a value ΔU_{Pt} of 1–5 mV.

To elucidate the influence of stirring on U_{Pt} we have performed additional experiments in a simple system $I^-/I_2/H_2O_2/H^+$ in which there are no instabilities. It has turned out that U_{Pt} is affected by stirring in such a simple system as well. However, at the relatively high I_2 concentration used (10^{-4}–10^{-6} M) this influence reveals itself only at extremely low concentrations of iodide (10^{-8}–10^{-10} M). As Re is increased the increment of the potential is obtained ($\Delta U_{Pt} \simeq$ 1–5 mV), and it the greater the lower the iodide concentration. This is explained by the change in the thickness of the diffusion layer at the electrode and by the rise in the diffusion potential (which depends on the distance between the Pt and the reference electrode) and is not associated with changes in the reagent concentrations in the reaction volume.

Hence we come to a conclusion that the influence of stirring on T_{ill} is due to microheterogeneities or nuclei of the new phase (II). Having ascertained this, we decided to test the effect of stirring on the oscillations as such. In this case the reaction was initiated at different Re values. The typical time dependences of A_{360} obtained under such conditions are shown in Figure 2. As can be seen, with increasing stirring intensity the oscillation amplitude and the duration of the oscillatory state increase by about 100% and 15–20%, respectively. A greater amplitude indicates that individual microvolumes in which oscillations take place are better synchronized at higher Re.

4. Results. Turbulence

In our experiments, the most pronounced changes in T_{ill} set in at $Re > 2000$. It is known[36] that the laminar-to-turbulent transition in long tubes also occurs at critical values $Re_{cr} \simeq 2000$. In reactors such as the one we use, the Re_{cr} value depends on the particular shapes of the vessel and stirrer; therefore to interpret the results obtained, one has to know the characteristics of liquid circulation in such a reactor. To obtain such characteristics, we have conducted two series of experiments.

In the first series, we have determined the dependences of the characteristic time t_{mix} of the mixing of a small drop of dye on the Re number. As follows from these data shown in Figure 8, such dependences are nicely described by a relation t_{mix} = constant·Re^{-n} where n = 1.24 for the mechanical stirrer and n = 2.3 for magnetic stirrer bars of different length. The $t_{mix}(Re)$ dependences display no inflections or distinctive marks of a laminar-to-turbulent transition. The only peculiarity in the case of the mechanical stirrer is that the last two points at high Re (>8000) drop out of the general dependence. This may be due to stirrer slipping (i.e., "idle strokes" entraining no liquid) at high rates ($f_0 \simeq$ 30 Hz), which can give rise to macroeddies rotating in the opposite direction and bubbles formed of entrapped air as well as of dissolved gas owing to cavitation. In all probability this is also the cause of the decline in the $H_{thr}(Re)$ dependence at $Re > 8000$ demonstrated in curves 1 and 2 of Figure 6.

It is noteworthy that when magnetic stirring bars of different length are used, the same t_{mix} is attained at different Re (confer curves 2 and 3 in Figure 8). Vice versa, at the same Re the t_{mix} values obtained with magnetic and mechanical stirrers differ several-fold. These examples serve to emphasize that the Reynolds number does not fully characterize the hydrodynamic state of the liquid throughout the reactor. Indeed, the flow velocity would not be the same in different points: at the rotation axis, or stirrer tip, near the reactor walls, bottom, or surface of the liquid.

Furthermore, the stirring efficiency in great measure depends not only on the linear dimensions of the stirrer but also on its cross-section area and shape. Figures 2 and 3 depict the results obtained with a glass-coated bar 1.8 cm long and 2 mm in diameter (Re = 5530 in curve 1 and Re = 11 300 in curve 2) and a Teflon-coated, embossed-surface bar 1.3 cm long and 8 mm in diameter (curves 3 and 4, Re = 5900); comparing, e.g., curves 2 and 4 one can see that T_{ill} is 3.6 times longer for a twice lower Re.

The data of Figure 8, the example above, and visual observation of the process of mixing of a drop testify to a rather complex rate distribution for liquid elements both in the vertical and in the radial directions, with chaotic pulsations and eddies superimposed on it.

This turbulent motion can be characterized by means of power spectra of flow velocities like the one shown in Figure 9. As can be seen, superimposed on a continuous spectrum typical of turbulent motion is a single line with a frequency of $2f_0$ (coefficient 2 stems from the stirrer having two blades). For the sake of simplicity the continuous spectrum can be characterized with a value $f_{1/3}$ which is determined from the relation $G(f_{1/3}) = {}^1/_3 G(0)$. The dependence of $f_{1/3}$ on f_0, which reflects the development of turbulence with increasing Re (for the mechanical stirrer $Re = 314 f_0$), is displayed in Figure 10, whence it follows that in the range $1500 < Re < 10\,000$ there are no inflections or irregularities of the curves that would mark an abrupt change in the hydrodynamic characteristics of liquid motion. Thus, we can

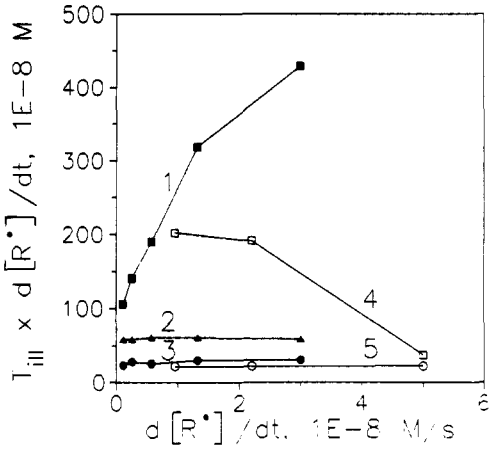

Figure 7. Dependences of the threshold integral concentration $[R^{\bullet}]_{thr}$ of radicals induced by light in T_{ill} ($R^{\bullet} = I^{\bullet}$, $R_xI^{\bullet}$) on their generation rate $d[R^{\bullet}]/dt$. Curves 1–3, blue light (12.8 mW) at respective *Re* of 11 300, 2280, and 1880; curves 4 and 5, white light (120 mW) at *Re* of 11 300 and 2010. Magnetic stirrer bars, t = 27 °C.

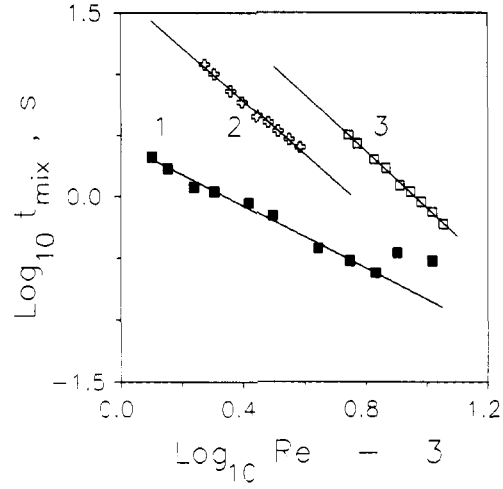

Figure 8. Dependences on *Re* of the characteristic time t_{mix} of the mixing of a drop of dye in water (V_0 = 10 mL). Curve 1, mechanical Teflon stirrer; curves 2 and 3, magnetic glass coated bars 2 mm in diameter and (2) 1.05 cm and (3) 1.8 cm long.

conclude that already from $Re \cong 2000$ up in our case the stirred liquid obeys the laws of developed turbulence.

5. Discussion

The following discussion is not aimed at rationalizing all the observations. We shall only consider the more general physical causes of the dependency of T_{ill} on stirring intensity, without attempting to interpret the exact profiles of the curves shown in Figures 4–7. We have presented experimental evidence that before the onset of the I → II transition in the homogeneous solution there appear microheterogeneities or nuclei of the new phase (II), i.e., microvolumes where the exponential increase in iodide starts earlier than in the bulk. Fluctuations in reagent concentrations may underlie the particular mechanism of nucleation.

In the preceding work[27] we showed that at $Re < 3000$ the observed dependence of T_{ill} on I_0 or (which is the same) on $d[R^{\bullet}]/dt$ (Figure 7) and the kinetics of the I → II transition starting from the moment of switching on the illumination are nicely described by the following equations:

$$d[I^-]/dt = \gamma[I^-] - k_0[In][I^-] + C(I_0) \quad (4)$$

$$d[In]/dt = -k_0[In][I^-] \quad (5)$$

where In is HOI or HIO_2, $k_0 \cong 10^8$–10^{11} M^{-1} s^{-1}, $C(I_0)$ is the photogeneration rate of radicals $R^{\bullet}$ that in subsequent reactions are converted to I^-; the initial concentrations $[In]_0$ and $[I^-]_0$ are 3×10^{-7} and 10^{-10} M, respectively. According to this simplified model, an autocatalytic rise in iodide sets in when the inhibitor concentration drops to a critical level $[In]_{cr} \cong \gamma/k_0 \cong 10^{-9}$–$10^{-12}$ M. Iodide-coupled reactions ensure an exponential increase in I_2 as well, with the same exponent γ.[26,27] As a result of fluctuations, autocatalysis may begin even at $[In]_v > [In]_{cr}$; this may happen in microvolumes (nuclei) where $[In]_n < [In]_{cr}$ (subscripts v and n refer the corresponding values to the total volume and the nucleus, respectively).

For microvolumes with a linear size of a few micrometers the relation $[In]_n < [In]_{cr}$ means the absence of inhibitor molecules in these microvolumes. Therefore to estimate the value V_1 for a microvolume in which nucleation would be most probable, it is necessary to calculate the maximal probability product $P_0(v)P_1(v)$, where $P_0(v)$ is the probability that the volume v does not contain a single In molecule and $P_1(v)$ is the probability that the volume v contains at least one iodide ion. Using the Poisson distribution for $P_0(v)$ and $P_1(v)$, we obtain

$$V_1 = ([I^-]_v N_A)^{-1} \ln (1 + [I^-]_v/[In]_v) \quad (6)$$

where N_A is the Avogadro number. For $[I^-]_v \cong [In]_v \cong [In]_{cr} \cong 10^{-10}$ M, from (6) we get $r_1 \equiv V_1^{1/3} \cong 2$ μm. Since on the strength of eq 5 events P_0 and P_1 are not statistically independent, the actual size can be expected to be somewhat greater than r_1.

The life time τ_n of a nucleus is strongly dependent on stirring, as it is determined by two opposite processes. On one hand, the nucleus develops owing to chemical reactions proceeding within it; on the other hand, the nucleus is destroyed by convection and pulsations that mix it with the bulk and by the inhibitor molecules coming in from the milieu. We shall first define the lifetime τ_m of certain isolated microvolumes as the time in which the distance r between its two particles (initially spaced by r_0) is doubled. If the size of such a microvolume does not exceed the minimal Kolmogorov size L_K[36] which is determined as

$$L_K \cong d\, Re^{-3/4} \quad (7)$$

(for a *Re* range 2000–12 000 the L_K ranges from 38 to 8.5 μm), then the time τ_m is set by the equation

$$\tau_m = (d/\Delta u)(L_K/d)^{2/3} \equiv (d/\Delta u)/Re^{1/2} \quad (8)$$

where Δu is the change in velocity u at distance d average over the entire volume.[36] To estimate Δu, let us make use of an expression for the time τ_v that is needed for two particles initially spaced by a distance λ_1 to move apart to a distance λ_2, provided that $\lambda_2 \gg \lambda_1 > L_K$:[36]

$$\tau_v \cong (\lambda_2^{2/3} d^{1/3})/\Delta u \quad (9)$$

If $\lambda_2 \cong d$, it can be assumed that $\tau_v \cong t_{mix}$; then $\Delta u \cong d/t_{mix}$. Substituting this expression in (8), we obtain

$$\tau_m \cong t_{mix} Re^{-1/2} \quad (10)$$

Using the data of Figure 8, we find that in the range of *Re* from 2000 to 12 000 the τ_m changes from 200 to 3 ms.

Let us now estimate how profoundly the chemical and photochemical reactions in the nucleus and mass transfer change the time τ_n as compared with τ_m. From eq 4 it follows that the rate of iodide formation in the nucleus owing to autocatalysis and photochemical reactions is determined by the sum $\gamma[I^-]_n + C(I_0)$. Meanwhile, the rate of the decline in $[I^-]_n$ is determined by mass transfer of iodide from and inhibitor into the nucleus. The amount j of a substance passing owing to turbulent diffusion through unit

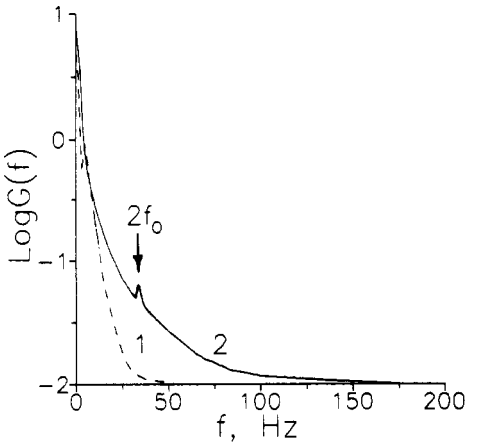

Figure 9. Typical power spectra of the photocurrent $G(f)$ obtained from a laser beam scattered on monodisperse 1.8-μm latex microspheres suspended in water and stirred with a mechanical stirrer at frequencies f_0 of 5.18 Hz (curve 1) and 17.8 Hz (curve 2). The scattering volume is situated midway between the cell center and wall.

surface area per unit time is set by the equation

$$j = \beta(c_n - c_v) \tag{11}$$

where the mass transfer coefficient β has the dimension cm/s, and c is concentration.[1] Consequently, the rate of change in the concentration of a substance in the nucleus owing to mass transfer is equal to $jS/\Delta V$ where S is the nucleus surface area and ΔV is its volume. For simplicity we shall assume that $S/\Delta V \cong 1/r_0$. Then the $[I^-]_n$ decline rate is determined as $(\beta/r_0)([In]_v + [I^-]_n - [I^-]_v)$. Further, since the rate constant of the reaction between I^- and In is close to the diffusion-controlled one, we assume that $[In]_n = 0$, and finally obtain

$$d[I^-]_n/dt = A[I^-]_n \tag{12}$$

where

$$A = \gamma + C(I_0)/[I^-]_n - (\beta/r_0)[In]_v/[I^-]_n - (\beta/r_0)([I^-]_n - [I^-]_v)/[I^-]_n \tag{13}$$

We believe that at $A > -(\tau_m)^{-1}$, τ_n begins to increase as compared with τ_m. At $A = 0$ the nucleus attains a state of unstable equilibrium and $\tau_n \to \infty$; in other words, having reached at $A = 0$ a critical size r_{cr} the nucleus does not disappear. To estimate r_{cr}, we shall first calculate β according to formula $\beta = St\,u$,[1] where St is the Stenton criterion. For turbulent motion the St value can be obtained as $St = 0.5Re^{1/2}Pr^{1/3}/Pe$,[1] where $Pr = \nu_k/D$ is the Prandtl number, $Pe = ud/D$ is the Peclet number, and D is the molecular diffusion coefficient, so that

$$\beta = 0.5Re^{1/2}Pr^{1/3}(D/d) \tag{14}$$

With Re changing from 3000 to 12 000, β changes from 2.2×10^{-3} to 5.5×10^{-3} cm/s. In estimating r_{cr} we should also bear in mind that at the moment of the I → II transition a linear increase in iodide becomes exponential (see Figure 1) and therefore the following relationship can be supposed to hold true at $A = 0$:

$$\gamma \cong C(I_0)/[I^-]_n \cong C(I_0)/[I^-]_v \tag{15}$$

Substituting (14) and (15) into (13) and assuming that at the moment of the I → II transition $[In]_v \cong [In]_{cr} \cong \gamma/k_0$, we find that

$$\beta\gamma/k_0C(I_0) \le r_c \ll \beta/\gamma \tag{16}$$

For $C(I_0) \cong (2\text{–}5) \times 10^{-8}$ M/s,[27] $\gamma \cong 0.3$ s^{-1}, $k_0 \cong 10^9$ M^{-1}/s^{-1} from (16), we obtain 0.1 μm $\le r_{cr} \ll$ 100 μm.

It should also be taken into account that an inequality $C_n(I_0) > C_v(I_0)$ may apply owing to selectively enhanced photon uptake by the nuclei;[37] this may be due, e.g., to a higher concentration of I_2 in the nucleus than in the milieu or to a higher extent of coupling between R_xI_2, $I^\bullet$, and I_2 in the nucleus.

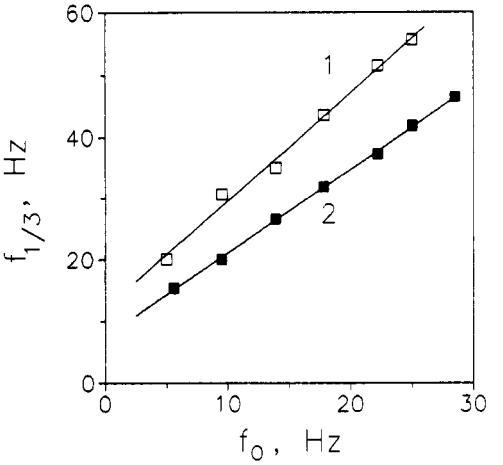

Figure 10. Dependences of the width $f_{1/3}$ of power spectra at one third of their height $G(0)$ on the frequency f_0 of the mechanical stirrer, for latex microspheres of diameter 0.7 μm (curve 1) and 1.8 μm (curve 2).

In conclusion, it must be noted that in systems like ours an important role in determining the threshold of "explosive" instability (and a decisive one for long-lived nuclei) is played by clusters, i.e., spatial formations of several nuclei.[38,39] In our case we can call long-lived the nuclei that move as a unity over a distance exceeding by far their own size r_0. In its lifetime τ_n the nucleus would be relatively displaced by a distance $l_0 = \Delta u\tau_n$; taking into account eqs 8 and the condition $\tau_m < \tau_n$, we can conclude that l_0 is not less than 200–400 μm. Such an estimate implies a high probability of cluster formation. In the clusters the increment in iodide may be significant, especially if their size approaches the critical value β/γ. Thereby cluster formation would shorten the time T_{ill}.

6. Appendix. The I → II Transition under Anaerobic Conditions

First of all it should be noted that oxygen evolution from the reaction mixture completely stops by the moment when absorbance at 360 nm reaches its maximum (see Figure 2). Therefore an increase of the Reynolds number cannot attenuate the extent of saturation of the solution with oxygen but, on the contrary, must enhance the rate of oxygen supply into the reactor from the air. As demonstrated experimentally, the time T_{ill} also increases with increasing Re, so oxygen—if somehow active—must inhibit the I → II transition. Conversely, anaerobiosis should diminish the T_{ill}.

To test the influence of O_2 on the kinetics of the I → II transition, we have conducted a series of experiments where the reaction solution has been purged with argon. In Figure 2, arrows tagged "Ar" mark the moments when argon was supplied into the reactor. Prior to switching on the illumination, the reactor has been purged with argon for 200 s, which is sufficient for at least a 10-fold decrease in dissolved $[O_2]$. In these experiments the reaction volume was 8 mL instead of the usual 10 mL and was stirred magnetically. With a glass-coated bar 2 mm in diameter and 1.8 cm long (Re = 11 300) we obtain $T_{ill} = 22 \pm 1$ s in aerobic conditions and $T_{ill}^{Ar} = 25.2$ s after argon purging; with a Teflon-coated bar 8 mm in diameter and 1.3 cm long (Re = 5900) the respective values are $T_{ill} = 76.2 \pm 1$ s and $T_{ill}^{Ar} = 88.2$ s. That is, the argon purge results in a slight (ca. 15%) increase in T_{ill} with both weak and vigorous stirring, whereas the profile of the dependence of T_{ill} on Re is not altered. This slight increase in T_{ill} may be due to additional stirring by the gas flow. Anyway,

no decrease in T_{ill} is observed upon removal of oxygen; consequently, the effect of stirring is not associated with the action of oxygen.

References and Notes

(1) Frank-Kamenetskii, D. A. *Diffuziya i teploperedacha v khimicheskoi kinetike* (*Diffusion and Heat Transfer in Chemical Kinetics*), 2nd ed.; Nauka: Moscow, 1967; 491 pp (Russian).

(2) Vavilin, V. A.; Zhabotinskii, A. M.; Zaikin, A. N. In: *Matematicheskie modeli biologicheskikh sistem* (*Mathematical Models of Biological Systems*); Frank, G. M., Ed.; Nauka: Moscow, 1971; pp 25–40 (Russian).

(3) Györgyi, L.; Field, R. J. *J. Phys. Chem.* **1989**, *93*, 2865–2867. Györgyi, L.; Rempe, S. L.; Field, R. J. *J. Phys. Chem.* **1991**, *95*, 3159–3165.

(4) Argoul, F.; Arneodo, A.; Richetti, P.; Roux, J. C. *J. Chem. Phys.* **1987**, *86*, 3325–3338.

(5) Schneider, F. W.; Kruel, Th.-M.; Freund, A. In: *Structure, Coherence and Chaos in Dynamical Systems*; Christiansen, Ed., Manchester, 1987.

(6) Luo, Y.; Epstein, I. R. *J. Chem. Phys.* **1986**, *85*, 5733–5740.

(7) Kumpinsky, E.; Epstein, I. R. *J. Chem. Phys.* **1985**, *82*, 53–57.

(8) Bar-Eli, K.; Noyes, R. M. *J. Chem. Phys.* **1986**, *85*, 3251–3257.

(9) Villermaux, J. In: *Spatial Inhomogeneities and Transient Behaviour in Chemical Kinetics*; Gray, P., Nicolis, G., Baras, F., Borckmans, P., Scott, S. K., Eds.; Manchester, U.K., 1990; p. 119.

(10) Horsthemke, W.; Hannon, L. J. *J. Chem. Phys.* **1984**, *81*, 4363–4368.

(11) Menzinger, M.; Jankowski, P. *J. Phys. Chem.* **1986**, *90*, 1217–1219.

(12) Ruoff, P. *Chem. Phys. Lett.* **1982**, *90*, 76–80.

(13) De Kepper, P.; Boissonade, J. In: *Fluctuations and Sensitivity in Nonequilibrium Systems*; Horsthemke, W., Kondepuri, D. K., Eds.; Springer: Berlin, 1984.

(14) Sevcik, P.; Adamcikova, I. *Chem. Phys. Lett.* **1988**, *146*, 419–421.

(15) Li, R. S.; Li, J. *Chem. Phys. Lett.* **1988**, *144*, 96–98.

(16) Menzinger, M.; Boukalouch, M.; De Kepper, P.; Boissonade, J.; Roux, J. C.; Saadaoui, H. J. *J. Phys. Chem.* **1986**, *90*, 313–315.

(17) Menzinger, M.; Giraudi, A. *J. Phys. Chem.* **1987**, *91*, 4391–4393.

(18) Menzinger, M.; Jankowski, P. *J. Phys. Chem.* **1990**, *94*, 4123–4126.

(19) Menzinger, M.; Dutt, A. K. *J. Phys. Chem.* **1990**, *94*, 4510–4515.

(20) Ochiai, E.-I.; Menzinger, M. *J. Phys. Chem.* **1990**, *94*, 8866–8868.

(21) Dutt, A. K.; Menzinger, M. *J. Phys. Chem.* **1990**, *94*, 4867–4870.

(22) Lopez-Tomas, L.; Sagues, F. *J. Phys. Chem.* **1991**, *95*, 701–705.

(23) De Kepper, P.; Horsthemke, W. In: *Synergetics Far from Equilibrium*; Springer Series in Synergetics; Pacault, A., Vidal, C., Eds.; Springer: Berlin, 1979; Vol. 3, p 61.

(24) Horsthemke, W.; Lefever, R. *Noise-Induced Transitions* Springer Series in Synergetics; Haken, H., Ed.; Springer: Berlin, 1984; Vol. 15; Chapter 7.2.

(25) Vanag, V. K. *J. Chem. Biochem. Kinet.*, in press.

(26) Vanag, V. K.; Schelyapin, A. A.; Alfimov, M. V. *Dokl. Akad. Nauk SSSR* **1991**, *316*, 388–391 (Russian).

(27) Vanag, V. K.; Alfimov, M. V. *J. Phys. Chem.*, previous paper in this issue.

(28) Nicolis, G.; Prigogine, I. *Self-Organization in Non-Equilibrium Systems*; Wiley-Interscience: New York, 1977.

(29) Polak, L. S.; Mikhailov, A. S. *Samoorganizatsiya v neravnoves nykh fiziko-khimicheskikh sistemakh* (*Self-Organization in Non-Equilibrium Physicochemical Systems*); Nauka: Moscow, 1983; 286 pp.

(30) Cook, D. O. *React. Kinet. Catal. Lett.* **1985**, *27*, 379–385.

(31) Furrow, S. D. *J. Phys. Chem.* **1989**, *93*, 2817–2823.

(32) *Photon Correlation and Light Beating Spectroscopy*; Cummins, H. Z., Pike, E. R., Eds.; Plenum: New York, 1974.

(33) Vanag, V. K.; Bakharev, V. N.; Eremeev, N. L.; Livshitz, V. A.; Gritzkova, I. A.; Kazanskaya, N. F.; Zubov, V. P.; Alfimov, M. V. *Bioteknologiya* **1989**, *5*, 729–734 (Russian).

(34) Semenov, N. N. *Tsepnye reaktsii* (*Chain Reactions*); ONTI: Leningrad, 1934; 360 pp (Russian).

(35) Furrow, S. D. *J. Phys. Chem.* **1982**, *86*, 3089–3094.

(36) Landau, L. D.; Lifshitz, E. M. *Teor. Fiz. Gidrodinamika* (*Theor. Phys. Hydrodynamics*), 4th ed.; Nauka: Moscow, 1988; 736 pp (Russian).

(37) Weigel, H., Plath, P. J. *Z. Phys. Chemie* (*Leipzig*) **1986**, *267*, 225–240.

(38) Mikhailov, A. S.; Uporov, I. V. *Zh. Eksp. Teor. Fiz.* **1980**, *79*, 1958–1972 (Russian).

(39) Mikhailov, A. S.; Uporov, I. V. *Zh. Fiz. Khim.* **1982**, *56*, 606–609 (Russian).